

Article

Assessment of a Coastal Aquifer in the Framework of Conjunctive Use of Surface Water and Groundwater—The Case of the River Nestos Western Delta, NE Greece

George Kampas ¹, Ioannis Gkiougkis ^{1,*} , Andreas Panagopoulos ² , Fotios-Konstantinos Pliakas ¹ and Ioannis Diamantis ¹

¹ Laboratory of Engineering Geology and Groundwater Research, Department of Civil Engineering, Democritus University of Thrace, 67100 Xanthi, Greece

² Hellenic Agricultural Organisation, Soil and Water Resources Institute, 57400 Sindos, Greece

* Correspondence: gkiougis@civil.duth.gr

Abstract: This paper presents research regarding the assessment of the hydrogeological system of the River Nestos Western Delta, NE Greece, during the period of 2019. The procedure included the collection and analysis of relevant hydrological and hydrogeological data concerning the aquifer system of the study area. Specifically, groundwater level measurements and sampling were carried out in a monitoring well network in the shallow unconfined and the deep confined aquifers of the study area, respectively; and surface water sampling was conducted from the River Nestos at selected locations in each of the main drainage canals, as well as in lagoons of the study area; followed by analysis and processing of the relevant chemical analyses results. Finally, piezometric, hydrochemical maps and diagrams were constructed to augment the evaluation of results and the assessment of the system. The present study contributes to the development and management of water resources in the River Nestos Delta area by providing insight into the hydrodynamic and hydrochemical status of the system based on comprehensive contemporary data that can support and justify the compilation of realistic measurements. The conjunctive management of the surface and groundwater in the study area can improve the quantitative and qualitative characteristics of the water. The water level in piezometric maps varies from -4 m up to 16 m for both time periods (May 2019 and October 2019). Moreover, the maximum values of EC are $2700 \mu\text{S}/\text{cm}$ and $2390 \mu\text{S}/\text{cm}$ for the confined and unconfined aquifer systems, respectively. The maximum values of Cl^- concentrations are $573.89 \text{ mg}/\text{L}$ for the confined aquifer system and $514.73 \text{ mg}/\text{L}$ for the unconfined aquifer system for both time periods (May 2019 and October 2019).

Keywords: hydrogeology; conjunctive use of surface water and groundwater; hydrochemical analysis; coastal aquifer management



Citation: Kampas, G.; Gkiougkis, I.; Panagopoulos, A.; Pliakas, F.-K.; Diamantis, I. Assessment of a Coastal Aquifer in the Framework of Conjunctive Use of Surface Water and Groundwater—The Case of the River Nestos Western Delta, NE Greece. *Hydrology* **2022**, *9*, 172. <https://doi.org/10.3390/hydrology9100172>

Academic Editor: Roohollah Noori

Received: 29 August 2022

Accepted: 27 September 2022

Published: 30 September 2022

Publisher's Note: MDPI stays neutral with regard to jurisdictional claims in published maps and institutional affiliations.



Copyright: © 2022 by the authors. Licensee MDPI, Basel, Switzerland. This article is an open access article distributed under the terms and conditions of the Creative Commons Attribution (CC BY) license (<https://creativecommons.org/licenses/by/4.0/>).

1. Introduction

Conjunctive use of surface water and groundwater is generally determined as the allotment of quantity and/or quality of surface water and groundwater so as to achieve one or more aims while satisfying certain limitations [1]. Conjunctive use of surface water and groundwater is regarded as the optimal beneficial practice that entails the coordinated and planned utilization of both surface and groundwater resources in order to satisfy water requirements in basins that are nearing their full water resources potential development [2]. Conjunctive use entails the designed and coordinated management of surface water and groundwater in order to maximize the efficiency of using the total water resources. Overall, a correctly managed integrated system will yield more water at a better economic rate than individually managed surface water and groundwater systems [3]. The different and supplementary characteristics, as well as the specificities of both surface water and groundwater, make it feasible to resolve specific requirements of

water quality and quantity in an efficient and financially viable manner by integrating the systems, rather than by managing them separately [4]. This is especially true in cases where surface and groundwater bodies are hydraulically interconnected; therefore, any possible contamination in one can also affect the other [3]. Moreover, groundwater is generally assumed to be a more reliable, and often higher quality, source of water compared to surface water, since it is normally less affected by dry spells or prolonged droughts, and more protected from accidental pollution events, remaining available during extreme climate events and/or incidental pollutant spillages [5,6].

As stated by [5], the conjunctive utilization of surface water and groundwater has been thoroughly studied and many techniques/methods for efficient water use planning and management are based on these studies [7–15].

To obtain sustainability, water resource systems ought to be designed and managed in such a way as to meet the socioeconomic needs of present and future generations, while preserving their ecological, environmental, and hydrological integrity [3]. Conjunctive management relates to labor planned at a basin level to optimize productivity, fairness, equity, and environmental sustainability by concurrently managing surface and groundwater resources in a systematized operation for the goal of ensuring that the full benefits of such a system outdo the sum of the benefits that would have resulted from an unorganized management of the separate components. In many cases, such a design is necessary to increase irrigation water for crop productivity [16].

The application of the conjunctive operation of surface and groundwater can achieve rational spatiotemporal allocation of water resources to enhance the utilization ratio of water resources and water supply ensured rate and apprehend the comprehensive treatment of water logging, drought, and alkalization [17,18].

A conjunctive utilization management study requires various data for geologic conditions, surface water resources, and groundwater resources; moreover, data for water utilization, distribution systems, and wastewater disposal are mandatory [2].

In the management framework of water resources in coastal and deltaic zones, irrigation by run-of-the-river applications, with improper management emerging as a result of intensive irrigation or increased groundwater exploitation, frequently results in waterlogging or seawater intrusion issues, respectively [1].

On the contrary, a conceptual model is defined as a simplified version of a real-world system [19,20]. Conceptual models are composed by including prime physical processes operating on simplified hydrogeological configuration within the generalized boundary conditions. The most critical step is to compile a comprehensive conceptual model. Such a model is the foundation of a groundwater model. The objective of the conceptual model is to clarify and simplify the field problem, thus organizing the associated field data, in order to analyze the system so that it can be more easily transformed into a numerical model at a later stage [21]. The conjugation of hydrogeological research and surveys involves the application of a number of methodologies in compiling a conceptual model containing basic exploratory data, hydrochemical typology, etc. [22]. New geodata are obtained through monitoring, and geographic information systems (GIS) supply functional tools using spatial analysis to process and compose information [23]. According to [24], GIS is an important tool in the development of a conceptual model for any groundwater flow and contaminate transport problem. GIS offers data management and spatial analysis capabilities that can be useful in groundwater modeling. It provides automatic data collection, systematic model parameter assignment, spatial statistics generation, and the visual display of model results, all of which can improve and facilitate modeling [25]. A precise conceptual model is directly related to an in-depth investigation of the physical system involving subsurface investigations (borehole logging, geophysical surveys, pumping tests, etc.), as well as hydrological (groundwater level monitoring, unsaturated zone study, etc.) and hydro-chemical measurements (in situ groundwater sampling and chemical analyses) [26]. According to [27], selecting the appropriate conceptual model for a given problem is one of the most important steps in the modelling process. The authors of [28] state that

the power of the groundwater model is determined by the conceptual model. Therefore, for assessing and reducing the risk of the model's prediction, the reliability analysis of the conceptual model is meaningful and necessary for groundwater simulation [29,30].

This paper presents research work regarding the conceptual model development of the hydrogeological system of the River Nestos Western Delta, NE Greece, as a prelude to organizing the conjunctive use of surface water and groundwater in the area. The procedure included the collection and analysis of relevant hydrological and hydrogeological data regarding the aquifer system of the study area. Processing and analysis of all the collected data revealed the key hydrodynamic evolution mechanisms of the system. It appears that one of the main advantages gained through the conjunctive use of surface water and groundwater in coastal areas would be to provide more surface water for irrigation using storage reservoirs and collective irrigation networks for controlling the overpumping of groundwater as a remedy for seawater intrusion.

2. Location of the Study Area

The study area is located at the eastern coastal part of the Prefecture of Kavala, NE Greece, and specifically occupies most of the western part of the River Nestos Delta (Figure 1). It is bounded by the River Nestos on the east and by the Aegean Sea on the south and west.

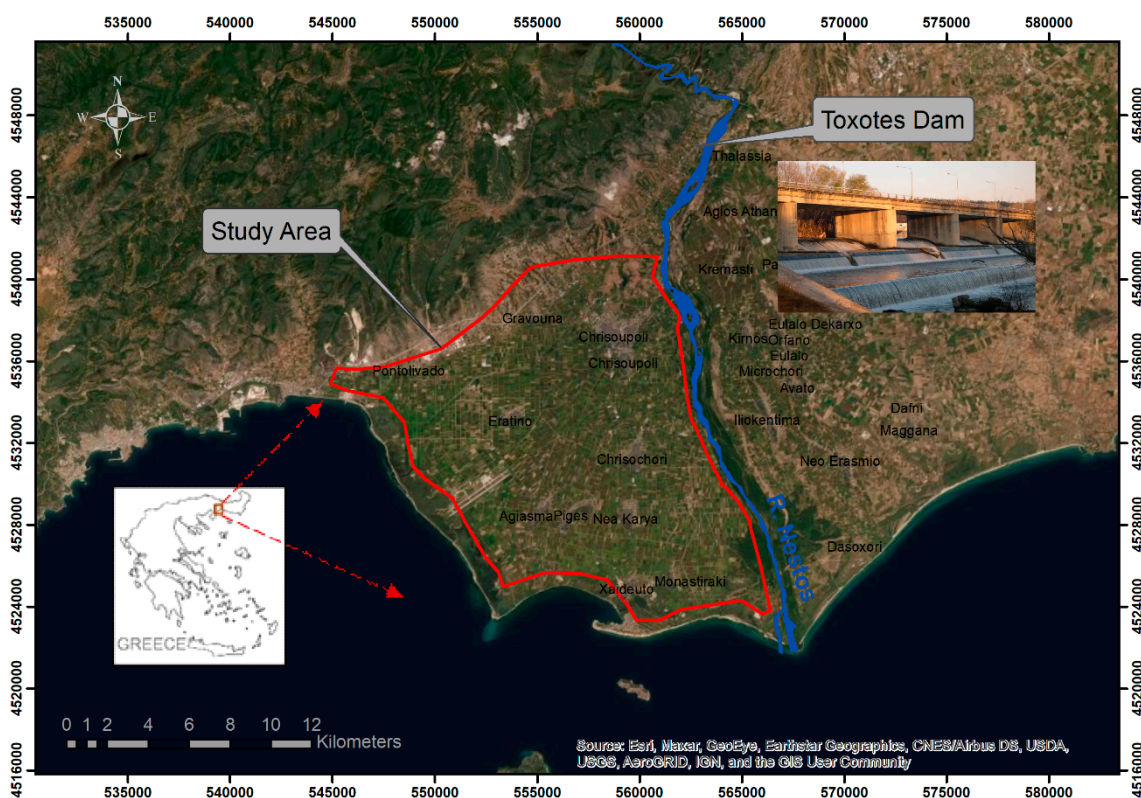


Figure 1. Study area (basemap source: Google, 2022).

The study area is part of the National Park of Eastern Macedonia and Thrace, which was established in 2008, and included the already protected areas of the Nestos Delta, Vistonida Lagoon, Ismarida Lagoon, and their wider area.

The lowland area of the Nestos River, which is essentially identical to the delta of the river, is bounded by the southern boundary of the Rhodope Mountain mass at the position of the Toxotes Dam and continues south down to the Thracian Sea coastline, including the entire length of the river from the dam to the sea. East and west, the delta spreads in about two equal parts from the villages of Nea Karvali to the west, up to Toxotes to the north and Avdira to the east.

The study area is a lowland area with mild slopes ranging from +40 m to 0 ± 1 m at the southern end of the coastline [31]. In this section, there are generally small morphological inclinations (<2%), from north to south, resulting in the formation of shallow sections that create seasonally stagnating surfaces (lakes or swamps). This feature, the marshes in particular, was the most prominent in earlier evolution phases of the delta and mainly owe their presence to the terminals of smaller secondary Nestos hills or mountain-zone currents [32].

3. Geological Setting

The deltaic area is formed of Holocene sediments with a thickness of some tens of meters deposited by the River Nestos and its sub-streams (Figure 2). These sediments consist alternately of clay, sand, and silt layering, reflecting a broad range of formational and depositional environments, producing a very diverse geological domain. In addition, due to delta marshes, the existence of organic clay is identified at some spots [26].

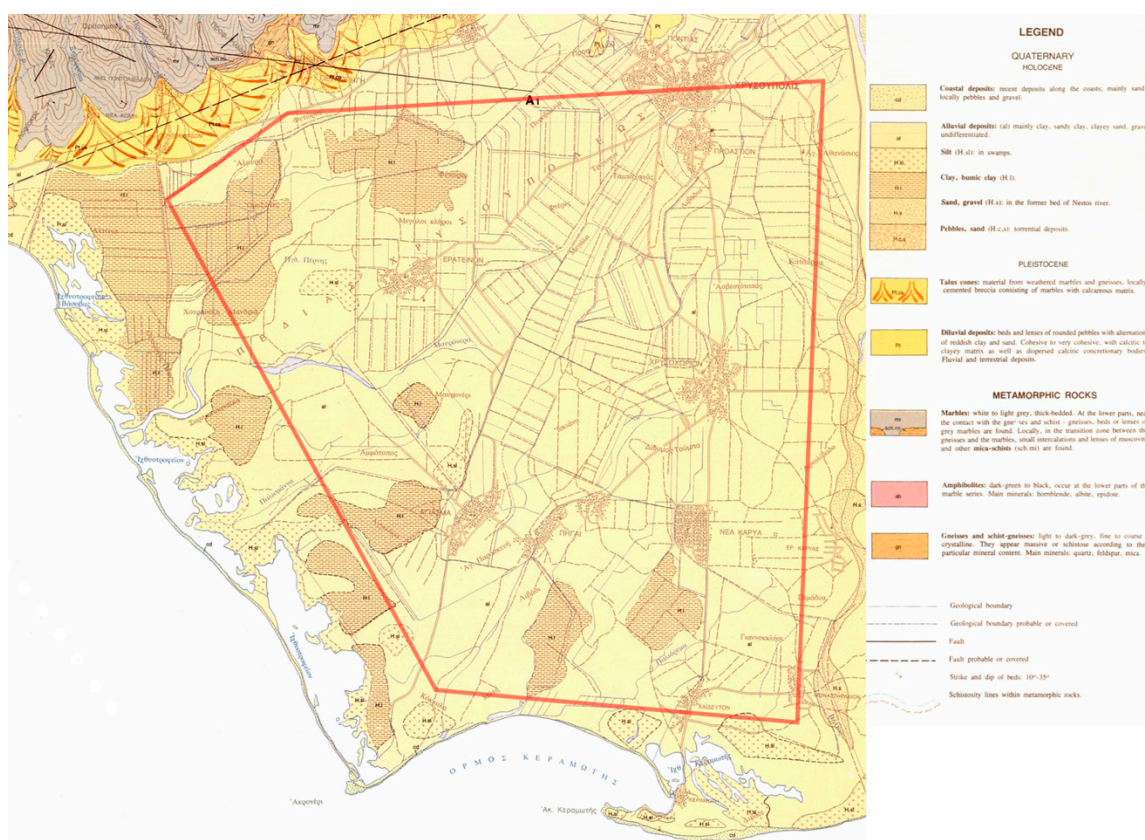


Figure 2. Geological map of the study area (outlined) [33].

The main study area belongs to the wider Nestos Delta region. The Nestos Delta is one of the most important wetlands in Greece, as well as Europe, due to the extent and diversity of its biotopes. It is included as one entry in the List of Wetlands of International Importance under the Ramsar Convention, belonging to the Natura 2000 network, as well as to the Special Protection Areas of Birds of the European Union. It is part of the National Park of Eastern Macedonia and Thrace, stretching from the Nestos Delta to the lagoons of Vistonida and Ismarida. In fact, the Nestos Delta consists of a mosaic of individual wetlands of which the largest and most distinct are the following (from D to A): The Bassova Lagoon, Eratinos Lagoon, Agiasmos Lagoon, Kokala Lagoon, Chaidou Lagoon, Keramoti Lagoon, Monastiraki Lagoon, and Magana Lagoon.

In the entire extent of the study area (~206 km²), most of the land use is agriculture (>77%). Flood irrigation is still practiced in large parts of the area, and this contributes

to groundwater recharge through deep percolation. Additionally, this process seems to contribute to the prevention of further seawater intrusion into the aquifer system, as groundwater abstractions are also limited. It is worth mentioning that currently, shallow wells are those which are used for irrigation purposes, while pumping from deep wells is very limited and occurs only for a short period of time during the irrigation season.

The entire amount of irrigation water comes from the Toxotes Dam (Figure 1). From this point, the two main canal routes (east and west) begin. Irrigation is carried out with open-type surface networks through reinforced concrete canals that cover an area of about 152,000 acres. In the rest of the region, at the present time, projects are being carried out to construct new irrigation canals to replace approximately 24,000 acres of existing earthen canals. Overall, collective surface irrigation networks serve the irrigation needs of approximately 176,000 acres. In the irrigated area of 176,000 acres, the water supply from the Toxotes Dam is facilitated by free flow irrigation (maximum quantity: $24 \text{ m}^3/\text{s}$), and flood irrigation is the main method practiced.

4. Hydrometeorological Conditions

Considering that the average annual rainfall value for the period of 1985–2019 is 496.80 mm, the total volume of precipitation in the study area, the spatial extent of which is 206.13 km^2 , is $102.40 \times 10^6 \text{ m}^3$.

The rainfall data presented in Figure 3 for the period, 2002–2019, comes from the Chrysoupolis meteorological station, which is situated in the town of Chrysoupolis (Figure 4). Specifically, Figure 3 shows the average monthly rainfall for the periods 2002–2007, 2008–2013, and 2014–2019.

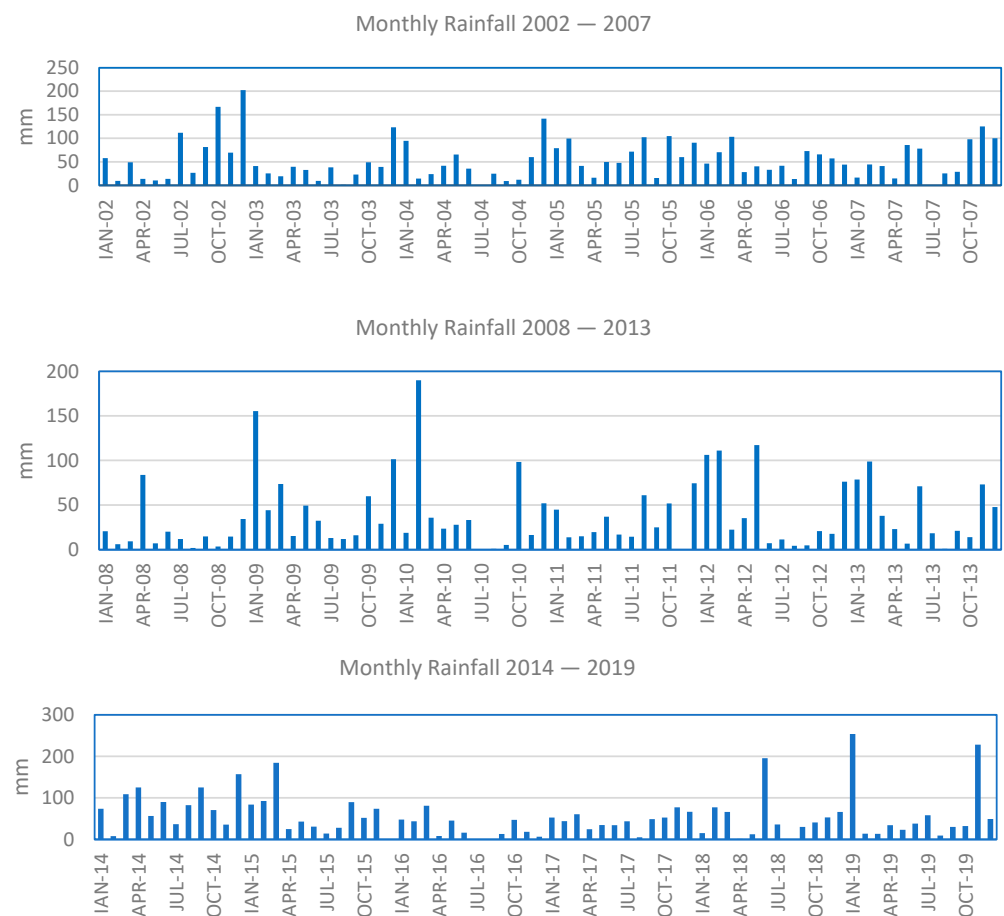


Figure 3. Monthly rainfall charts from Chrysoupolis meteorological station.

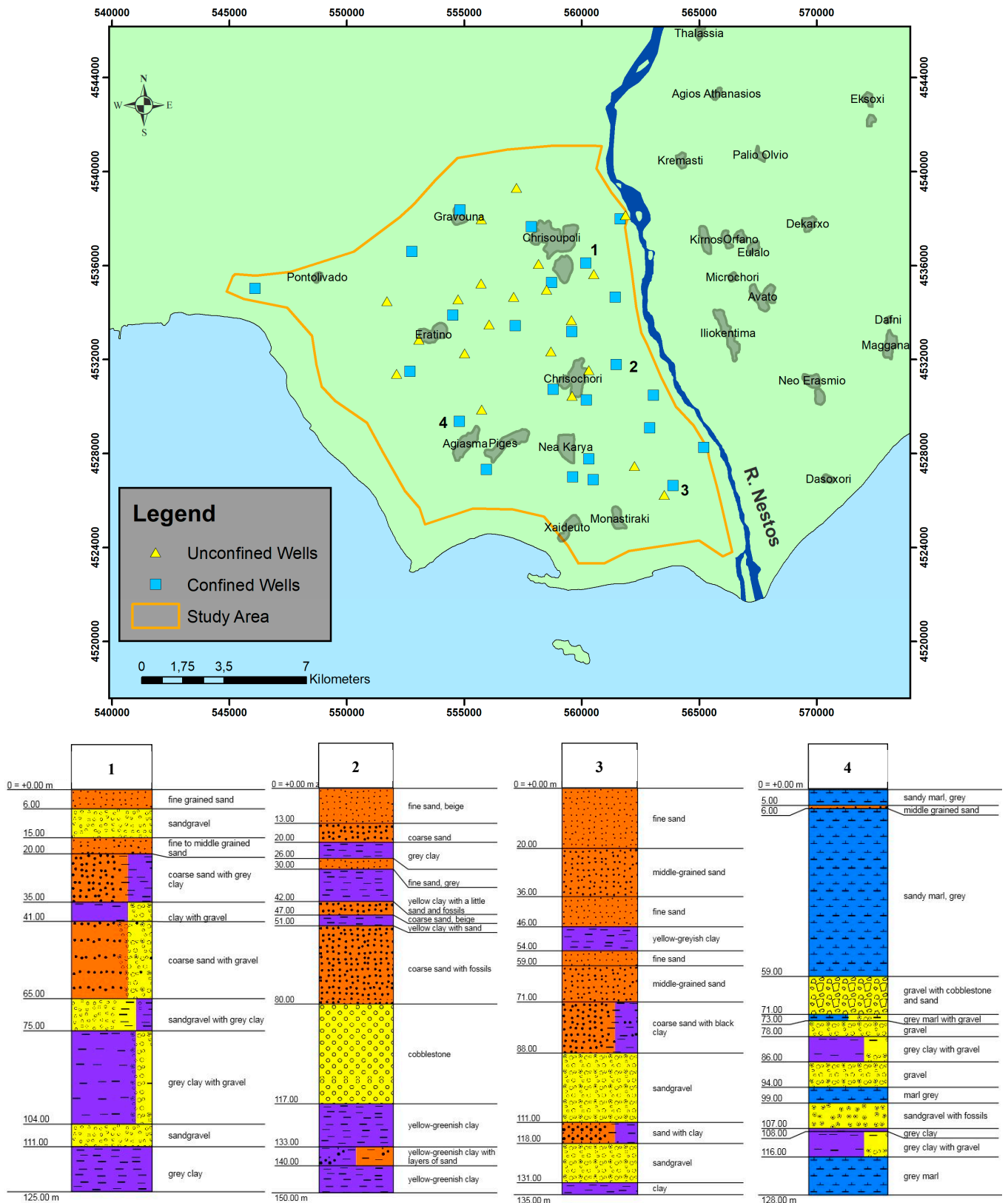


Figure 4. Upper: groundwater monitoring network points. Lower: geological sections of confined wells 1, 2, 3, 4, the positions of which are shown in the upper map.

An analysis of the presented data yields the following results:

1. The average annual rainfall is 496.80 mm. The minimum and maximum annual rainfall are 227.30 mm and 968.20 mm, respectively, for the same period.
2. The peak value of rainfall is observed in November and December. The period of July–September contains the months with the minimum rainfall values.

5. Hydrogeological Setting

In the area of the Nestos River Delta, two water-reserve zones are developing: (a) the zone of the unconfined aquifer and (b) the zone of the confined aquifer, located in the range of the Miocene series.

The first zone is directly recharged by precipitation, percolation through the Nestos riverbed, and lateral crossflows from the karst system of the wider area along the northern boundary of the studied system. Lateral crossflows mainly contribute to the recharge of the aquifers of the Miocene series. In the Quaternary deposits of the delta plain, the unconfined aquifer is formed, which is currently characterized by limited groundwater level fluctuation [25].

In the western part of the Nestos River Delta, according to earlier reports, the first zone of the aquifer system had begun to weaken. This zone experienced a great decline in the observed groundwater level in shallow wells over the years. There are two main reasons for this phenomenon: overpumping and the construction of lined canals. In addition, the construction of some deep drainage canals created a continuous discharge from the unconfined aquifer.

The second zone of the confined aquifer is made up of the permeable formations of the delta (gravel, sands), which alternate with clays, in the vertical as well as in the horizontal dimension, forming superimposed aquifers. Below the unconfined aquifer, there are other aquifers up to a depth of 150 m. Among these confined aquifers, some are artesian and are detected from a depth of about 15 m. These artesian aquifers have been located at depths of up to 120 m in the area of Keramoti [34].

The irrigation network in the study area, with water supply from the River Nestos, was constructed during the 1950s. Comparison of older hydrological and hydrogeological data to the monitoring data collected in the framework of this study demonstrate that groundwater levels in the study area have recovered considerably, and consequently, quality indicators have improved over the last 20 years and especially after the operation of the dams constructed by the Greek Public Power Corporation (PPC) at the upstream portions of the River Nestos. This is due to the fact that surface water, instead of groundwater, has been used for irrigation purposes in the study area since 2000, thus enabling the aquifer system to recover to its baseline state, before systematic abstractions were initiated.

In the present research in the study area, two networks of groundwater monitoring points were created (Figure 4). One network includes monitoring wells focusing on the unconfined aquifer, with a depth of less than 15 m, and the other is comprised of monitoring wells that focus on the confined aquifer, with a depth of more than 75 m. Figure 4 presents the geological sections of four selected wells in the confined aquifer. Piezometric maps were designed based on the relevant groundwater level measurements for the four time periods of May to October 2019 (Figures 5–8).

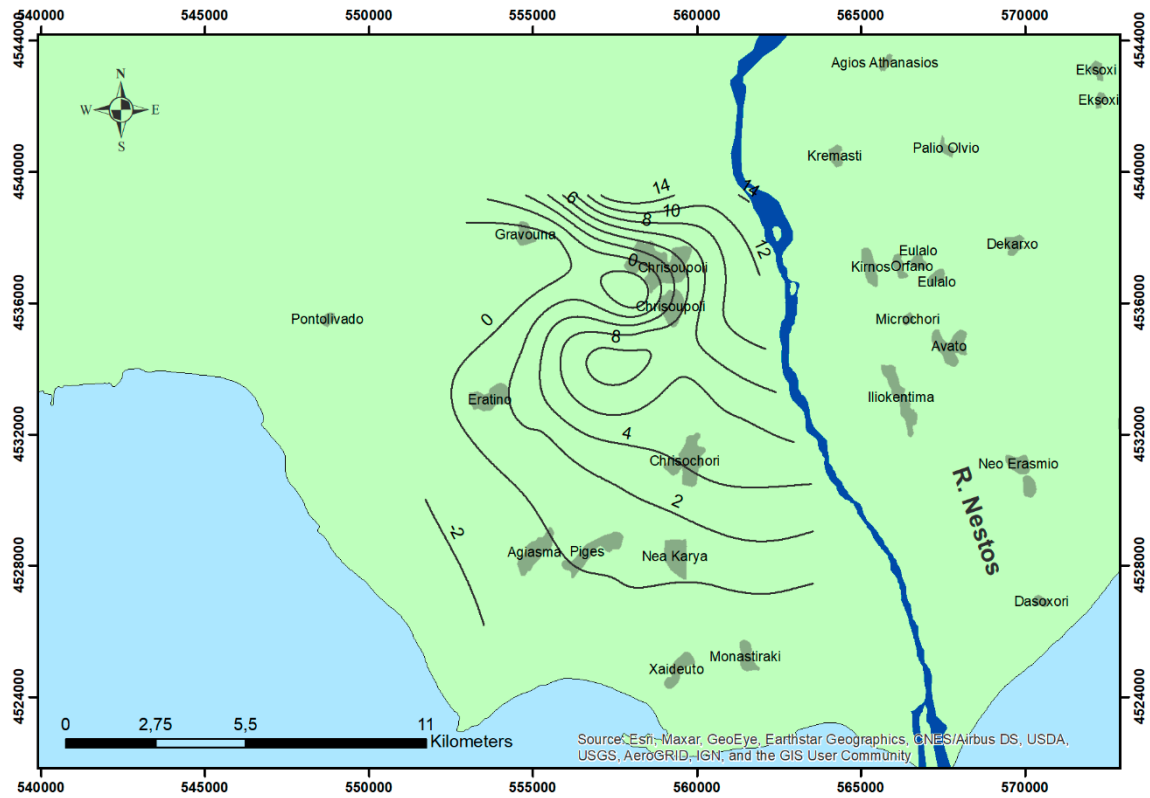


Figure 5. Piezometric map of the unconfined aquifer (May 2019).

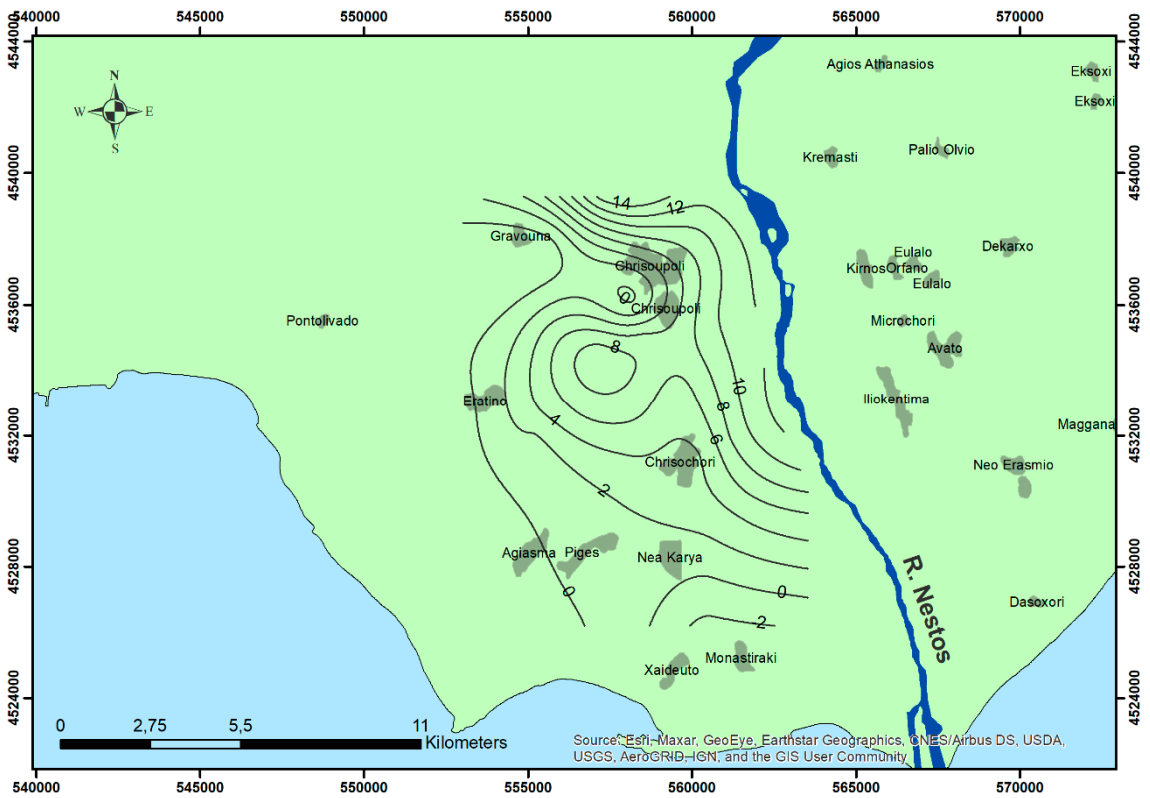


Figure 6. Piezometric map of the unconfined aquifer (October 2019).

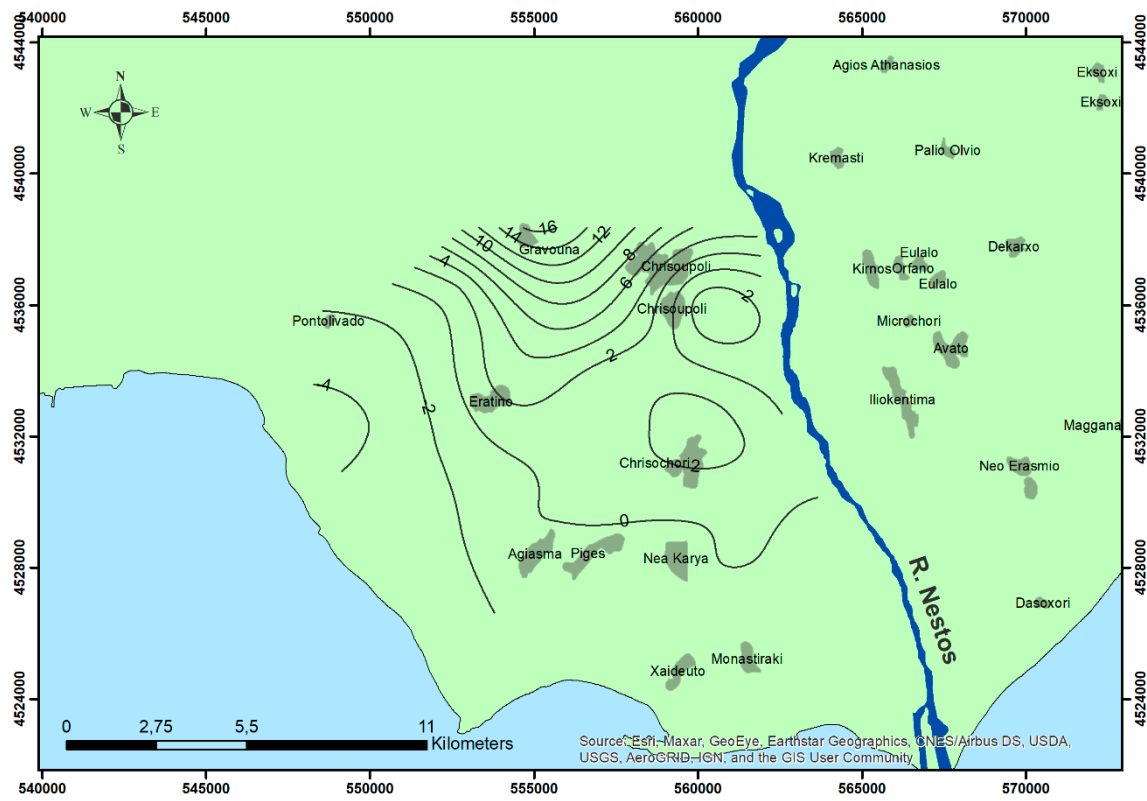


Figure 7. Piezometric map of the confined aquifer (May 2019).

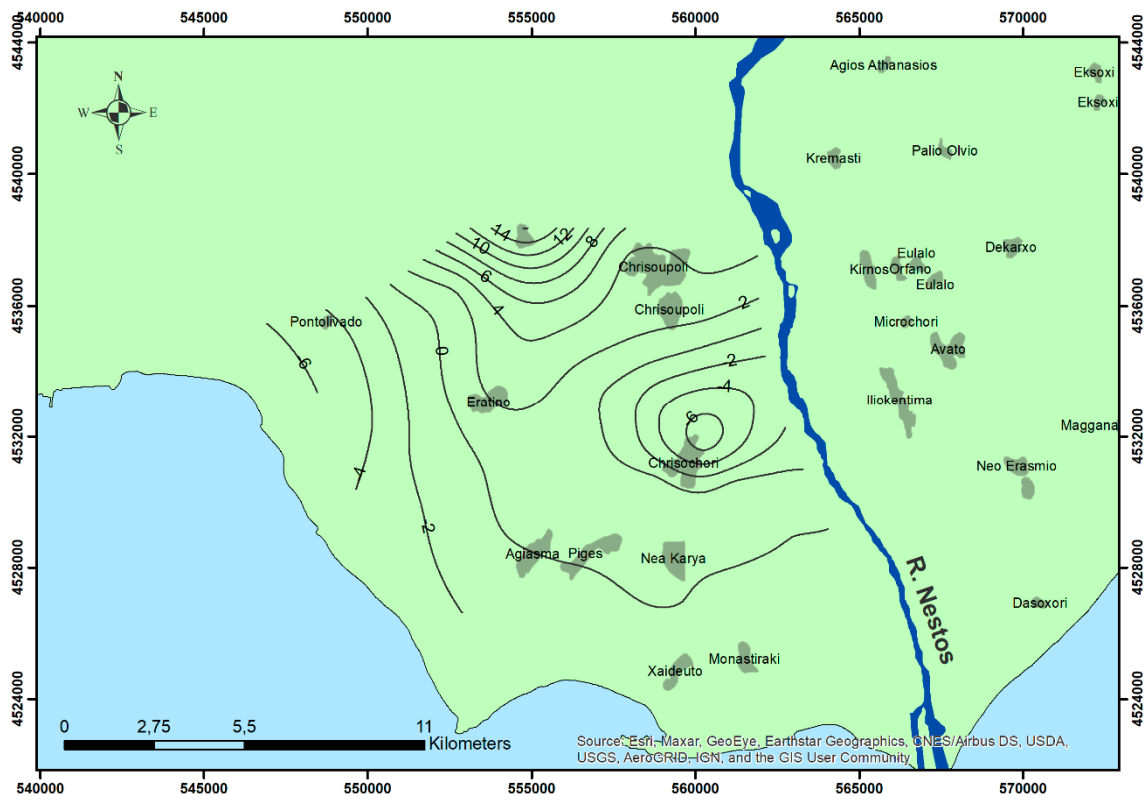


Figure 8. Piezometric map of the confined aquifer (October 2019).

After analyzing these maps, the following conclusions were drawn:

1. The main groundwater recharge areas of the upper unconfined aquifer system occur mainly from the N-NW portion of the study area from the River Nestos and old riverbeds, as well as from the local irrigation network.
2. There were no significant groundwater level fluctuations detected in either the confined or unconfined aquifers during the four periods.

6. Hydrochemical Setting

In the framework of this research work, in situ measurements of groundwater temperature, pH, and electrical conductivity were performed. In addition, groundwater sampling from 24 and 22 wells from the unconfined and the confined aquifers, respectively, in the study area was carried out in two time periods (May and October 2019). Then, relevant chemical analyses were performed at the accredited laboratory of the Soil and Water Resources Institute-Hellenic Agricultural Organization, Sindos, Greece. The laboratory measurements included the determination of several physicochemical and chemical parameters such as: temperature, pH, electrical conductivity, alkalinity, NH_4^+ , NO_3^- , NO_2^- , Cl^- , Na^+ , Ca^{2+} , Mg^{2+} , Mn^{2+} , Fe^{2+} , SAR, total hardness, and SO_4^{2-} . Hydrochemical maps were also compiled, presenting the spatial distribution of temperature, pH, electrical conductivity, NH_4^+ , NO_3^- , NO_2^- , Cl^- , Na^+ , Ca^{2+} , Mg^{2+} , Mn^{2+} , Fe^{2+} , SAR, and SO_4^{2-} values. In Figures 9–16, the spatial distributions of electrical conductivity and Cl^- values are presented. In Tables 1–4, the statistical analysis results of some of the major chemical constituents from groundwater samples obtained in May and October 2019 are tabulated.

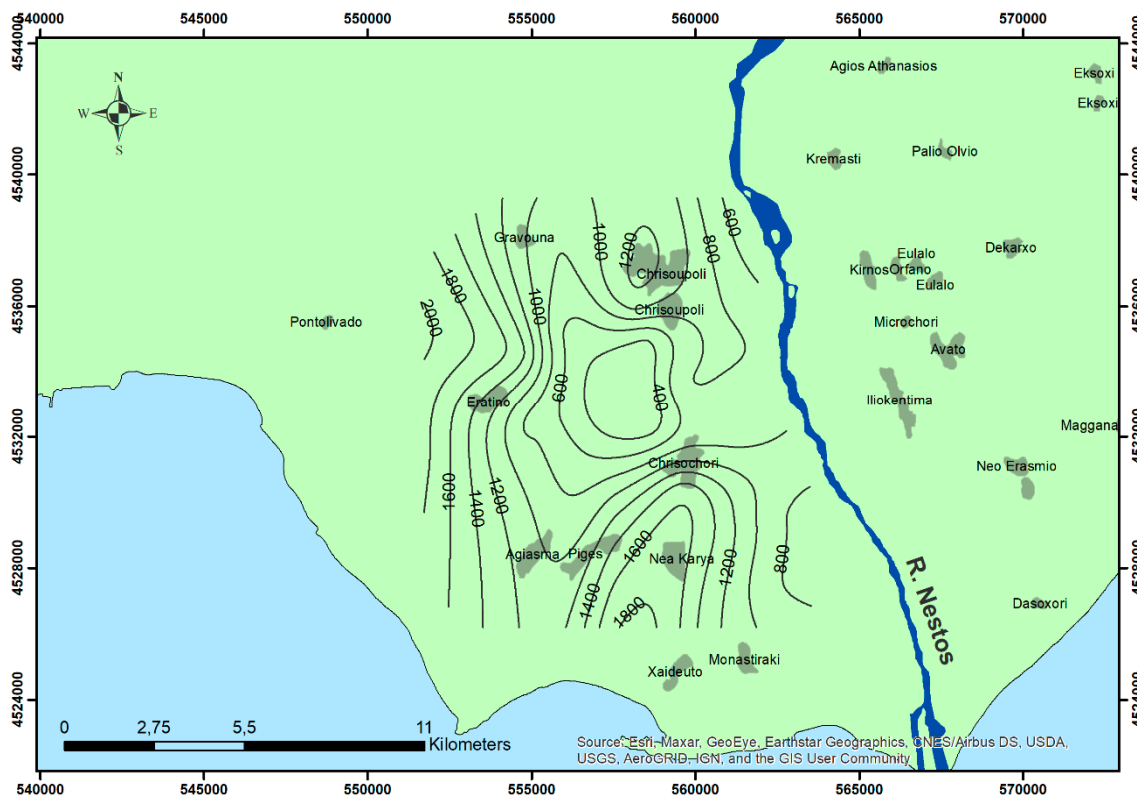


Figure 9. Electrical conductivity distribution map ($\mu\text{S}/\text{cm}$) of the unconfined aquifer (May 2019).

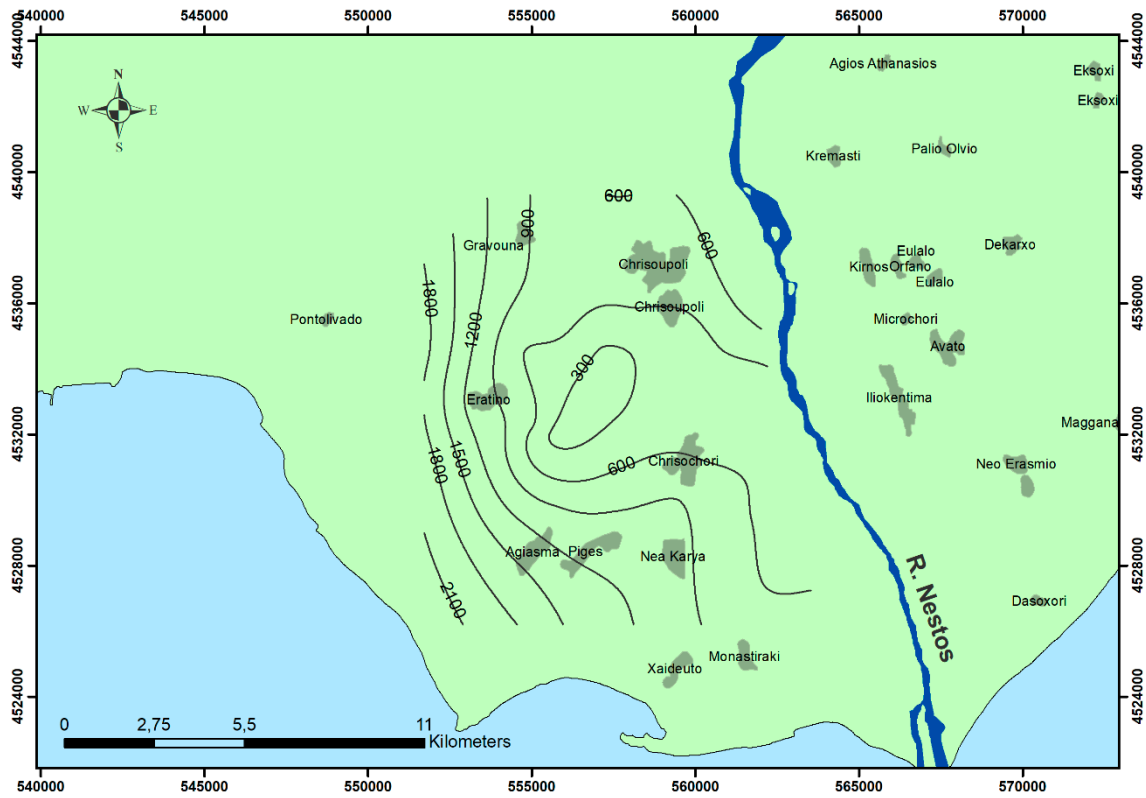


Figure 10. Electrical conductivity distribution map ($\mu\text{S}/\text{cm}$) of the unconfined aquifer (October 2019).

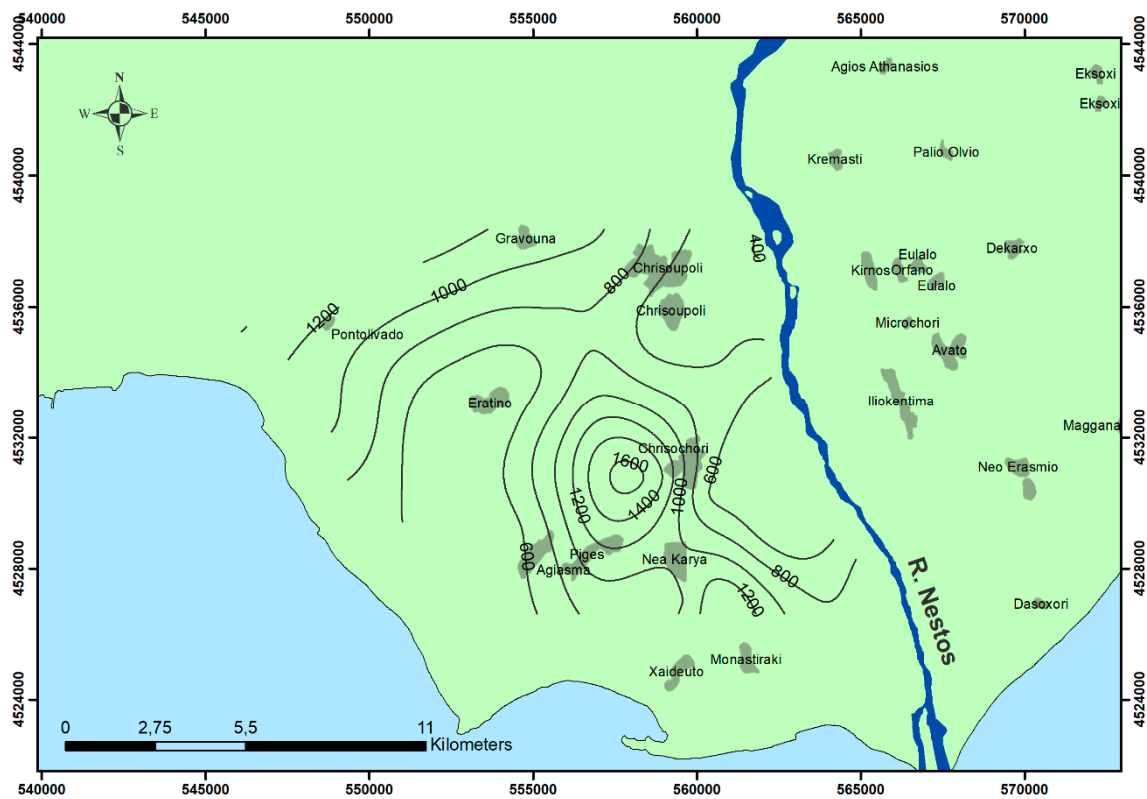


Figure 11. Electrical conductivity distribution map ($\mu\text{S}/\text{cm}$) of the confined aquifer (May 2019).

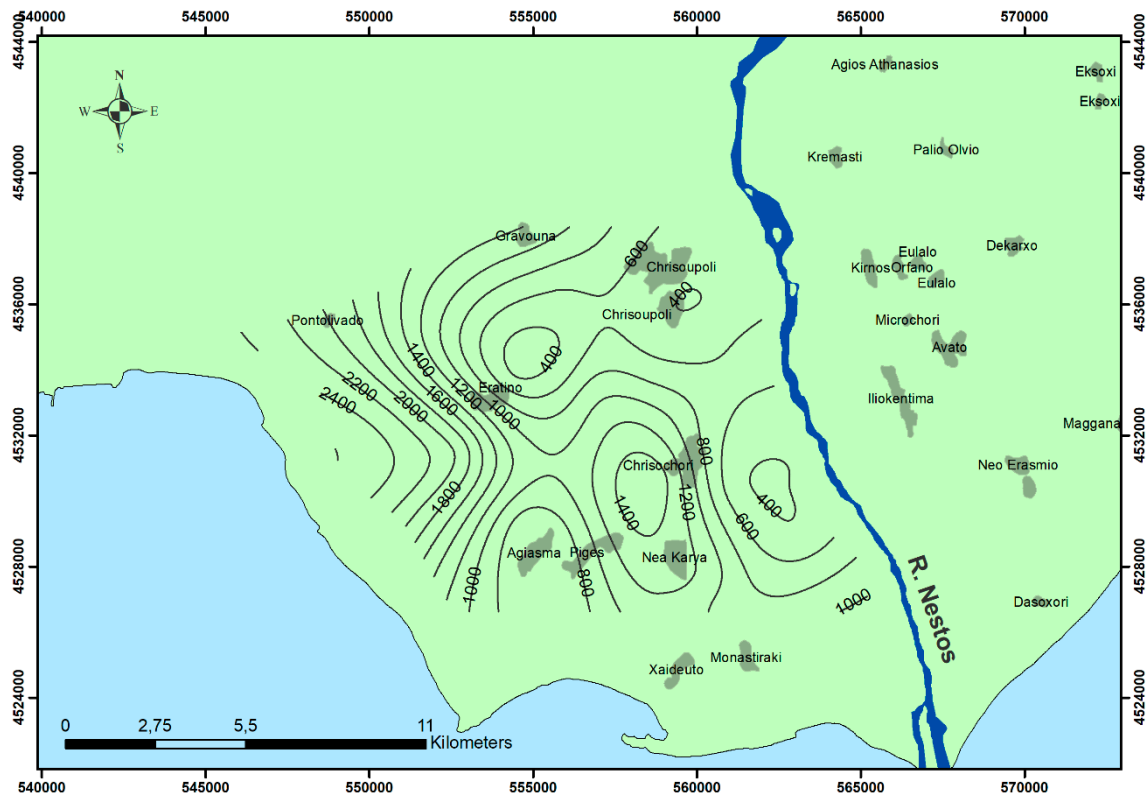


Figure 12. Electrical conductivity distribution map ($\mu\text{S}/\text{cm}$) of the confined aquifer (October 2019).

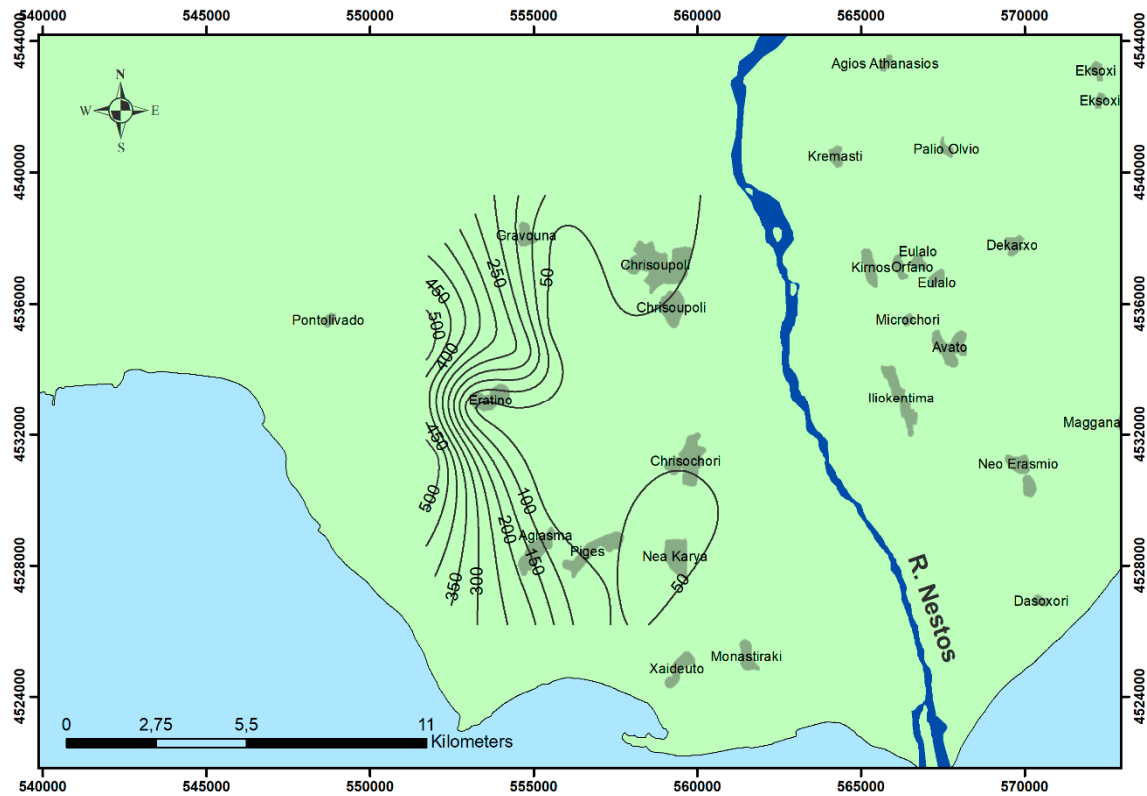


Figure 13. Chloride ion (Cl^-) distribution map (mg/L) of the unconfined aquifer (May 2019).

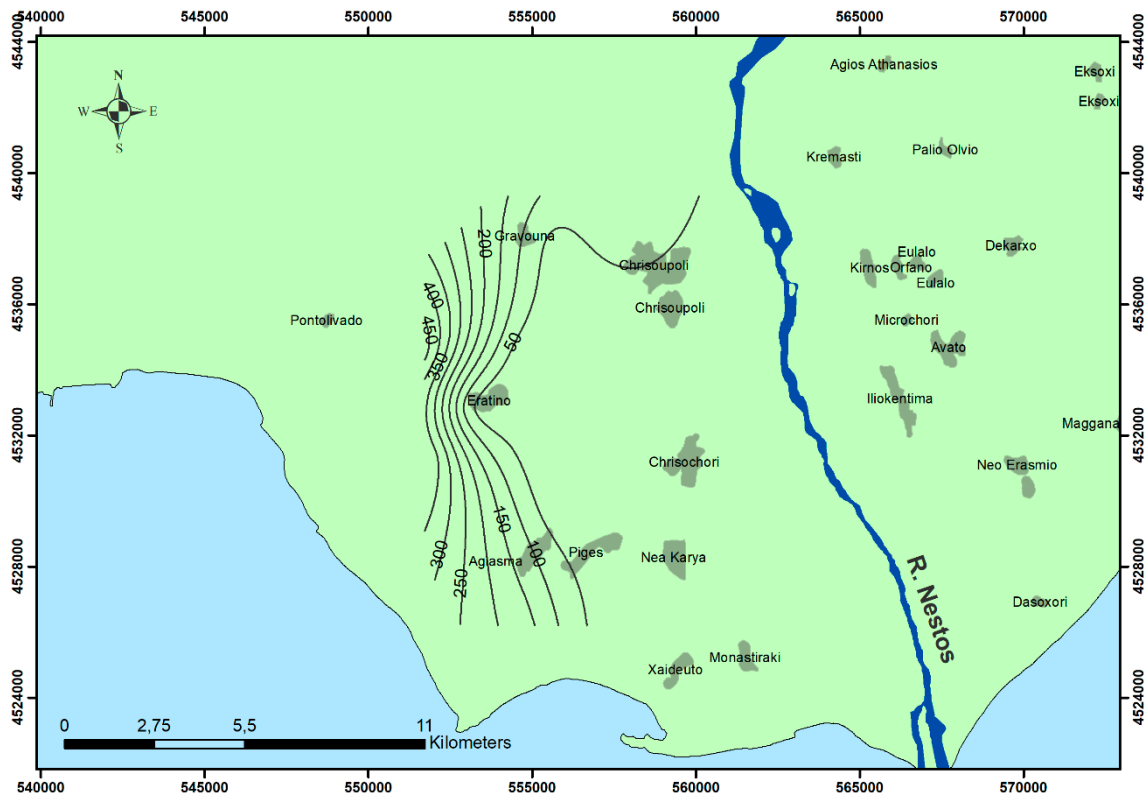


Figure 14. Chloride ion (Cl^-) distribution map (mg/L) of the unconfined aquifer (October 2019).

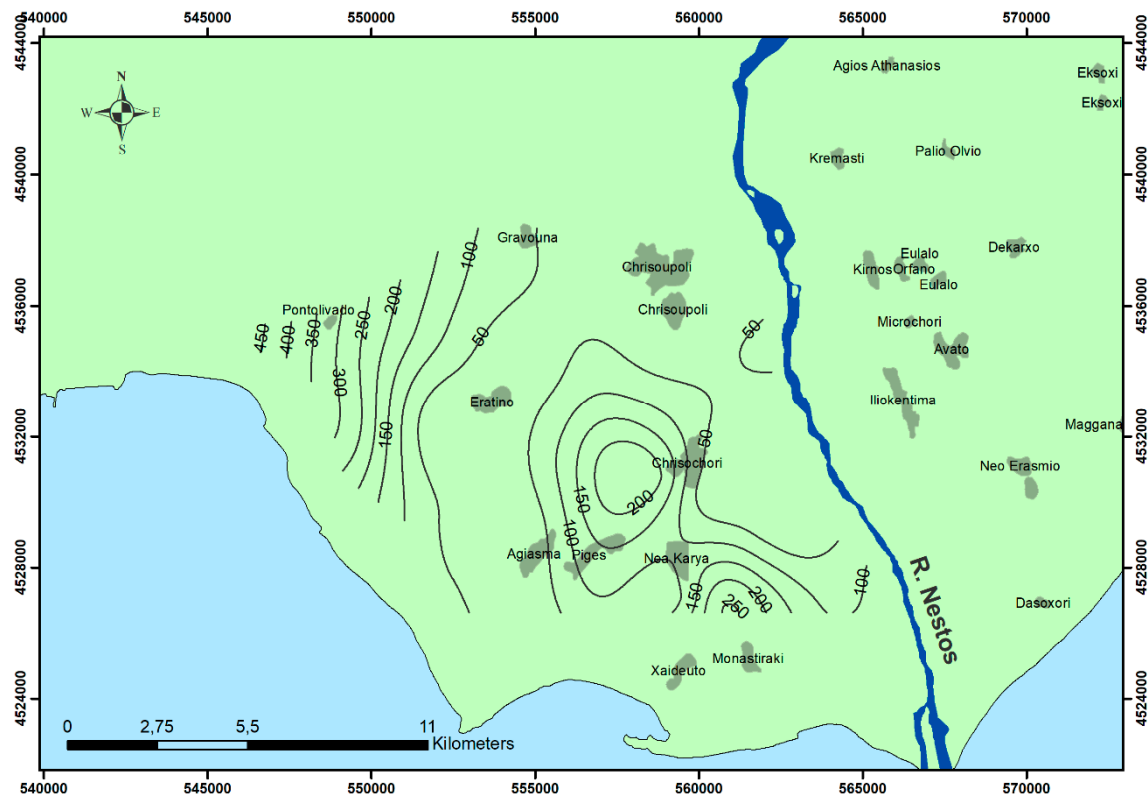


Figure 15. Chloride ion (Cl^-) distribution map (mg/L) of the confined aquifer (May 2019).

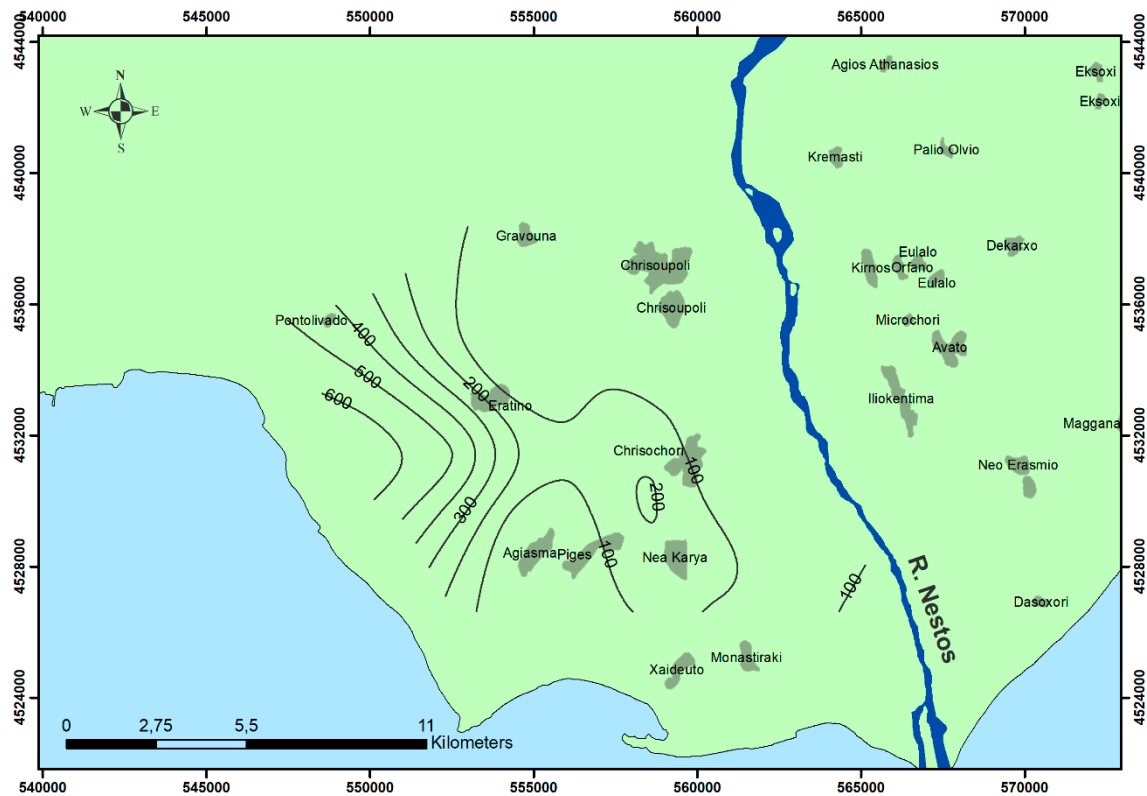


Figure 16. Chloride ion (Cl⁻) distribution map (mg/L) of the confined aquifer (October 2019).

Table 1. Statistical analysis of some of the major chemical constituents from groundwater samples (May 2019) (unconfined aquifer).

	Ca ²⁺ (mg/L)	Mg ²⁺ (mg/L)	SO ₄ ²⁻ (mg/L)	HCO ₃ ⁻ (mg/L)	NO ₃ ⁻ (mg/L)	Cl ⁻ (mg/L)	EC (μS/cm)	pH	Temp. (°C)	Na ⁺ (mg/L)	Fe ²⁺ (mg/L)	Mn ²⁺ (mg/L)
min	24.28	6.80	0.00	53.47	0.00	5.84	335.00	6.87	14.80	7.06	0.00	0.00
max	176.90	43.35	151.55	620.84	61.66	514.73	2390.00	7.46	24.30	364.72	853.60	2740.20
aver	99.86	20.33	49.22	387.65	9.75	71.14	924.95	7.15	17.86	77.03	59.64	1011.41
SD	37.82	10.87	49.44	139.86	15.85	126.93	527.01	0.15	2.11	94.55	182.40	759.57

Table 2. Statistical analysis of some of the major chemical constituents from groundwater samples (May 2019) (confined aquifer).

	Ca ²⁺ (mg/L)	Mg ²⁺ (mg/L)	SO ₄ ²⁻ (mg/L)	HCO ₃ ⁻ (mg/L)	NO ₃ ⁻ (mg/L)	Cl ⁻ (mg/L)	EC (μS/cm)	pH	Temp. (°C)	Na ⁺ (mg/L)	Fe ²⁺ (mg/L)	Mn ²⁺ (mg/L)
min	0.41	0.73	0.00	240.09	0.00	4.11	388.00	6.80	17.30	16.64	0.00	6.65
max	120.25	52.20	97.22	644.43	140.50	484.15	2590.00	8.20	22.50	331.85	234.60	1544.40
aver	45.79	13.25	16.99	386.50	10.80	88.32	907.70	7.42	19.59	127.10	53.02	476.15
SD	36.46	11.71	26.83	99.05	32.07	107.84	497.55	0.38	1.37	99.99	74.10	456.60

Table 3. Statistical analysis of some of the major chemical constituents from groundwater samples (October 2019) (unconfined aquifer).

	Ca ²⁺ (mg/L)	Mg ²⁺ (mg/L)	SO ₄ ²⁻ (mg/L)	HCO ₃ ⁻ (mg/L)	NO ₃ ⁻ (mg/L)	Cl ⁻ (mg/L)	EC (μS/cm)	pH	Temp. (°C)	Na ⁺ (mg/L)	Fe ²⁺ (mg/L)	Mn ²⁺ (mg/L)
min	21.12	6.05	0.00	124.01	0.00	4.78	320.00	7.13	17.00	6.72	12.02	9.64
max	145.80	40.75	163.05	595.88	44.68	461.37	2080.00	8.37	26.30	278.12	338.50	1856.00
aver	90.58	20.07	51.24	363.28	9.48	60.04	820.43	7.45	18.91	65.29	66.27	756.34
SD	29.94	11.37	41.95	113.22	12.09	118.23	449.42	0.25	1.91	76.02	87.53	506.95

Table 4. Statistical analysis of some of the major chemical constituents from groundwater samples (October 2019) (confined aquifer).

	Ca ²⁺ (mg/L)	Mg ²⁺ (mg/L)	SO ₄ ²⁻ (mg/L)	HCO ₃ ⁻ (mg/L)	NO ₃ ⁻ (mg/L)	Cl ⁻ (mg/L)	EC (μS/cm)	pH	Temp. (°C)	Na ⁺ (mg/L)	Fe ²⁺ (mg/L)	Mn ²⁺ (mg/L)
min	1.66	0.77	5.00	200.70	0.00	4.05	394.00	7.14	17.10	13.65	11.28	9.12
max	174.20	54.00	125.77	698.01	126.00	573.89	2700.00	8.36	20.70	481.63	545.60	1135.00
aver	56.22	13.47	25.70	397.99	9.96	102.95	936.71	7.68	19.09	135.31	67.49	408.14
SD	47.97	11.95	35.69	115.64	29.37	150.92	589.89	0.33	1.02	126.84	119.21	343.00

Moreover, in situ measurements of surface water temperature, pH, and electrical conductivity were performed, and surface water sampling was performed in three monitoring sites along the River Nestos course (Nestos 1, 2, and 3) and in four monitoring sites on the main drainage canals (T1, T2, T3, and T4) in the study area (Tables 5–8) for the same time periods (May and October 2019) (Figure 17). Relevant laboratory measurements regarding the surface water sampling included the determination of several physicochemical and chemical parameters such as: temperature, pH, electrical conductivity, alkalinity, NH₄⁺, NO₃⁻, NO₂⁻, Cl⁻, Na⁺, Ca²⁺, Mg²⁺, Mn²⁺, Fe²⁺, SAR, total hardness, and SO₄²⁻.

Table 5. Data of the major chemical constituents from the main four drainage canals (May 2019).

	Ca ²⁺ (mg/L)	Mg ²⁺ (mg/L)	SO ₄ ²⁻ (mg/L)	HCO ₃ ⁻ (mg/L)	NO ₃ ⁻ (mg/L)	Cl ⁻ (mg/L)	EC (μS/cm)	pH	Temp. (°C)	Na ⁺ (mg/L)	Fe ²⁺ (mg/L)	Mn ²⁺ (mg/L)
T1	60.70	7.40	19.22	204.88	4.96	12.05	389.00	7.65	21.20	13.24	11.60	23.82
T2	65.60	8.95	7.76	227.88	2.83	11.21	432.00	7.59	20.70	14.42	13.40	144.90
T3	53.85	6.45	6.13	189.08	4.29	7.99	362.00	7.64	20.70	10.40	11.69	68.67
T4	56.55	6.40	9.22	187.43	2.25	5.68	337.00	7.42	20.40	6.57	53.58	47.46

Table 6. Data of the major chemical constituents from the main four drainage canals (October 2019).

	Ca ²⁺ (mg/L)	Mg ²⁺ (mg/L)	SO ₄ ²⁻ (mg/L)	HCO ₃ ⁻ (mg/L)	NO ₃ ⁻ (mg/L)	Cl ⁻ (mg/L)	EC (μS/cm)	pH	Temp. (°C)	Na ⁺ (mg/L)	Fe ²⁺ (mg/L)	Mn ²⁺ (mg/L)
T1	66.05	9.05	18.85	250.08	5.02	14.93	462.00	7.91	17.10	15.89	19.39	<6.52
T2	70.30	10.60	22.85	265.39	2.99	13.97	499.00	7.89	18.30	19.87	<10.00	9.99
T3	62.80	8.25	21.58	248.17	5.43	9.93	426.00	7.90	17.60	12.91	<10.00	6.77
T4	59.10	7.00	8.13	201.29	2.37	5.16	355.00	7.81	16.40	8.15	19.51	7.58

Table 7. Data of the major chemical constituents from the Nestos River (May 2019).

	Ca ²⁺ (mg/L)	Mg ²⁺ (mg/L)	SO ₄ ²⁻ (mg/L)	HCO ₃ ⁻ (mg/L)	NO ₃ ⁻ (mg/L)	Cl ⁻ (mg/L)	EC (μS/cm)	pH	Temp. (°C)	Na ⁺ (mg/L)	Fe ²⁺ (mg/L)	Mn ²⁺ (mg/L)
Nestos 1	72.90	7.45	<5.00	234.61	3.07	5.78	397.00	7.41	18.4	4.45	<10.00	19.95
Nestos 2	49.40	5.15	<5.00	160.39	2.18	4.69	291.00	7.86	20.4	5.10	<10.00	10.42
Nestos 3	53.20	5.60	<5.00	164.43	2.18	4.90	302.00	7.88	21.0	5.20	30.20	18.20

Table 8. Data of the major chemical constituents from the Nestos River (October 2019).

	Ca ²⁺ (mg/L)	Mg ²⁺ (mg/L)	SO ₄ ²⁻ (mg/L)	HCO ₃ ⁻ (mg/L)	NO ₃ ⁻ (mg/L)	Cl ⁻ (mg/L)	EC (μS/cm)	pH	Temp. (°C)	Na ⁺ (mg/L)	Fe ²⁺ (mg/L)	Mn ²⁺ (mg/L)
Nestos 1	61.60	6.45	<5.00	187.00	2.84	4.84	351.00	7.67	17.00	5.36	11.62	9.79
Nestos 2	50.20	5.65	<5.00	175.00	2.17	5.08	305.00	8.16	18.10	6.16	<10.00	<6.52
Nestos 3	51.45	5.70	5.22	177.00	2.29	4.21	307.00	8.22	19.10	6.36	14.33	12.25

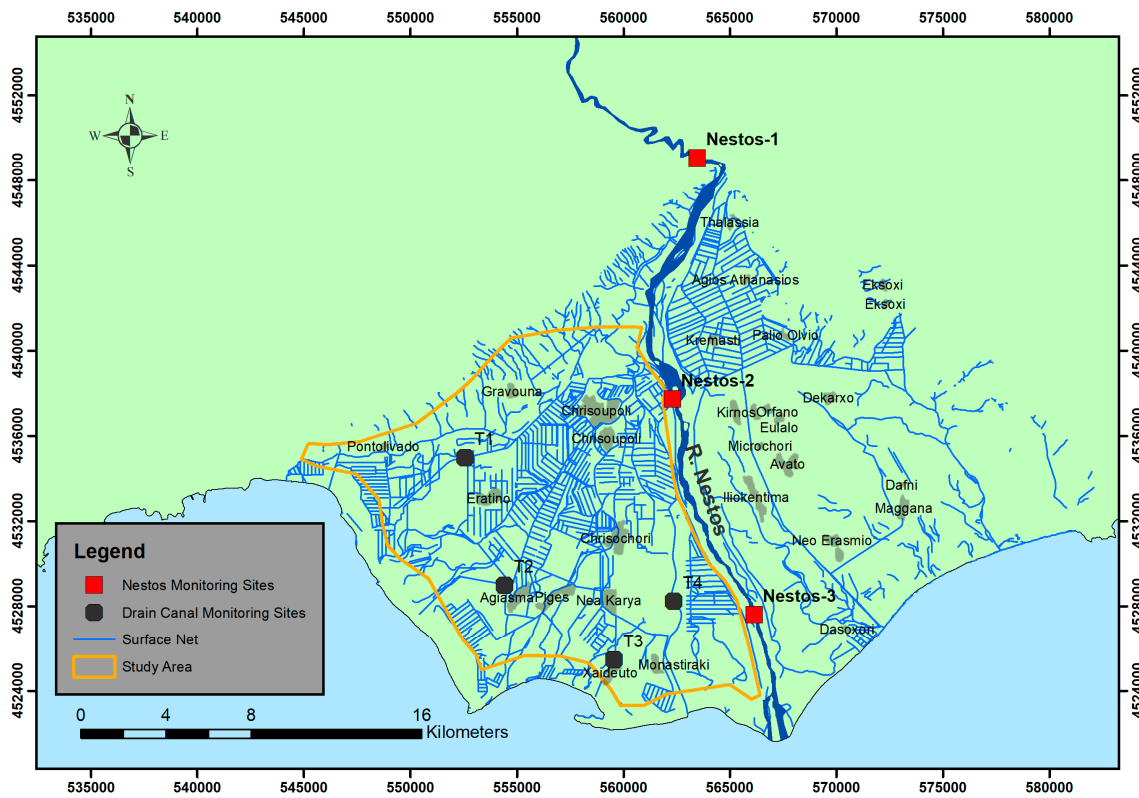


Figure 17. Surface monitoring network points.

From the analysis of the Piper and Durov diagrams (Figures 18 and 19), for both the confined and the unconfined aquifers, it is concluded that most of the samples are in the range of magnesium bicarbonate type, and some of the samples show mixed type behaviors [35].

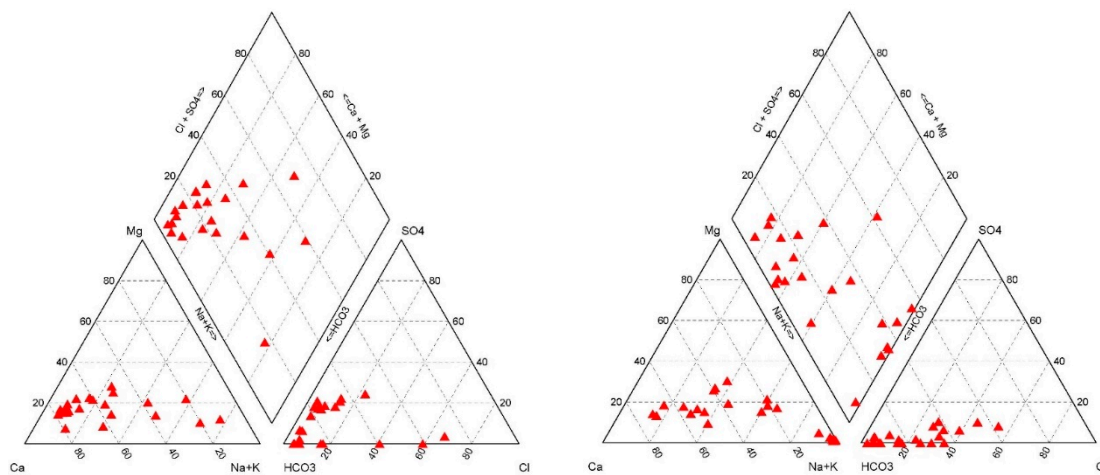


Figure 18. Trilinear Piper diagrams for the groundwater samples from the unconfined (left) and confined (right) aquifer of the study area (May 2019).

The EC values range from 388 $\mu\text{S}/\text{cm}$ to 2700 $\mu\text{S}/\text{cm}$ for the confined aquifer system and from 320 $\mu\text{S}/\text{cm}$ to 2390 $\mu\text{S}/\text{cm}$ for the unconfined aquifer system for both time periods. The highest values are observed in both the unconfined and the confined aquifer in the western and southern portions of the study area. This fact was expected because these are the areas closest to the sea, and they are more susceptible to the seawater intrusion phenomena.

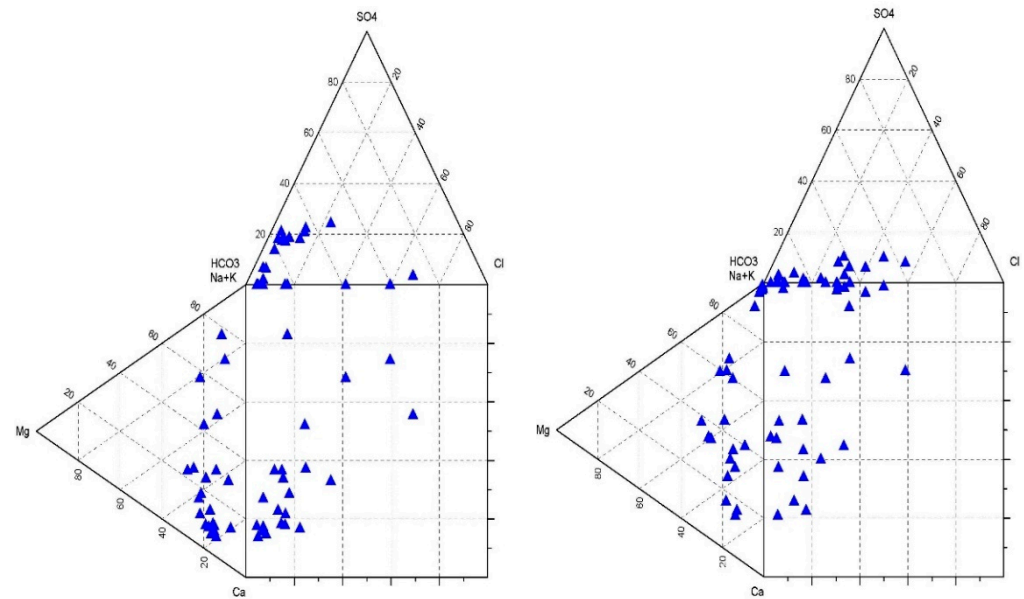


Figure 19. Durov diagrams for the groundwater samples from the unconfined (left) and confined (right) wells of the study area (May 2019).

The values of Cl^- concentrations range from 4.05 mg/L to 573.89 mg/L for the confined aquifer system and from 4.78 mg/L to 514.73 mg/L for the unconfined aquifer system for both time periods. These values are observed mainly in the western part of the study area and in wells that are adjacent to the sea and away from the River Nestos.

The values of NO_3^- concentrations range from 0.00 mg/L to 140.50 mg/L for the confined aquifer system and from 0.00 mg/L to 61.66 mg/L for the unconfined aquifer system for both time periods, with most values being around 10.00 mg/L for all monitoring wells and for all seasons. In general, most values are below 50.00 mg/L, which is the maximum admissible concentration for human consumption, and it is commonly used as a threshold value for the purpose of assessing the chemical status of groundwater bodies in Greece.

None of the values of all measured parameters at the four sampling points of the drainage canals for all periods show exceedances, according to relevant national hydro-chemical regulations for irrigation and potable water. Particularly, the maximum value of EC was 499.00 $\mu\text{S}/\text{cm}$, with a minimum value of 337.00 $\mu\text{S}/\text{cm}$. Moreover, the maximum value of NO_3^- was 5.43 mg/L in the drainage canal T3 for the period October 2019, while the values of Cl^- were >5.16 mg/L for all canals and for all periods.

Finally, it must be noted that most isolines are obtained automatically from the GIS interpolation software.

7. Conclusions

The area of the western part of the River Nestos Delta plays an important role in the economic development and the environmental balance of the broader area. In the area, two water-reserve zones are developing: (a) the zone of the unconfined aquifer and (b) the zone of the confined aquifer located in the ranges of the Miocene series, the first zone of the aquifer. According to earlier reports, this area had begun to weaken. Over the years, this zone has faced a significant lowering in the observed groundwater level in shallow wells. Two main reasons were identified for this phenomenon: overpumping and the construction of concealed canals. On the contrary, the construction of some deep drainage canals created a continuous discharge to the unconfined aquifer. The second zone of the confined aquifer is hosted in the permeable formations of the delta (gravel, sands) that alternate with clays.

For the purposes of the present research, two networks of groundwater sampling points were created in the study area. One network included wells of the unconfined

aquifer, with a depth of less than 15 m, and another well network was made up of the confined aquifer, with a depth of more than 75 m. Piezometric maps were designed based on the relevant groundwater level measurements for the four time periods (May and October of 2019, respectively).

In the framework of this research, groundwater level measurements, including in situ measurements of groundwater temperature, pH, and electrical conductivity, and groundwater sampling from 24 and 22 wells from the unconfined and the confined aquifer, respectively, at the study area were carried out in two time periods (May and October 2019). Moreover, in situ measurements of surface water also took place, which included temperature, pH, and electrical conductivity, as well as surface water sampling from three monitoring sites in the Nestos River and in four monitoring sites on the main drainage canals of the study area for the same time periods. Laboratory measurements included determination of temperature, pH, electrical conductivity, alkalinity, NH_4^+ , NO_3^- , NO_2^- , Cl^- , Na^+ , Ca^{2+} , Mg^{2+} , Mn^{2+} , Fe^{2+} , SAR, total hardness, and SO_4^{2-} . Hydrochemical maps were also compiled presenting the spatial distribution of several parameters.

The processing and analysis of all the collected data resulted in significant findings with regards to the hydrodynamic evolution of the system, where one of the main advantages of the conjunctive use of surface water and groundwater in coastal areas appears to be the provision of more surface water irrigation, with the help of storage reservoirs and irrigation networks, for controlling the overpumping of groundwater as a remedy for seawater intrusion.

Furthermore, the present study is expected to contribute to the development and management of water resources in the eastern and western delta of the River Nestos, where two different methods of using irrigation water occur. In addition, it is considered that the results of this research can enrich the database emerging from the transfer of surface water from the River Nestos planned for the irrigation of a total area of more than 200 km².

As surface water has been used intensively for irrigation for the last 20 years, the conjunctive management of surface water and groundwater is very interesting for further study. Relevant measurements should be continued in order to assess how the use of surface water can improve the quantitative and qualitative characteristics of groundwater [36].

Finally, the goal of this study was to establish a solid conceptual model for the study area in the framework of hydrogeological investigation regarding the conjunctive use of water, without a need of a detailed approach for each contributing factor. An additional, more detailed approach is planned as a future stage for this research.

Author Contributions: Conceptualization and methodology, G.K. and I.G.; writing—original draft preparation, review, and editing, G.K., I.G. and F.-K.P.; validation and supervision, A.P., F.-K.P. and I.D. All authors have read and agreed to the published version of the manuscript.

Funding: This research received no external funding.

Data Availability Statement: The study did not report any data.

Acknowledgments: The results of the paper are part of the research of the doctoral dissertation (last stage of Ph.D.).

Conflicts of Interest: The authors declare no conflict of interest.

References

1. Rao, S.V.N.; Bhallamudi, M.; Thandaveswara, B.S.; Mishra, G.C. Conjunctive Use of Surface and Groundwater for Coastal and Deltaic Systems. *J. Water Resour. Plan. Manag.* **2004**, *130*, 255–267. [[CrossRef](#)]
2. Todd, D.K.; Mays, L.W. *Groundwater Hydrology*, 3rd ed.; John Wiley & Sons, Inc.: New York, NY, USA, 2005.
3. De Wrachien, D.; Fasso, C.A. Conjunctive use of surface and groundwater: Overview and perspective. *Irrig. Drain.* **2002**, *51*, 1–15. [[CrossRef](#)]
4. Sahuquillo, A. Conjunctive use of surface water and groundwater. UNESCO encyclopedia of life-support systems. *Groundwater* **2002**, *3*, 206–224.
5. Zhang, X. Conjunctive surface water and groundwater management under climate change. *Front. Environ. Sci.* **2015**, *3*, 59. [[CrossRef](#)]

6. Kundzewicz, Z.W.; Doll, P. Will groundwater ease freshwater stress under climate change? *Hydrol. Sci. J.* **2009**, *54*, 665–675. [[CrossRef](#)]
7. Ejaz, M.S.; Peralta, R.C. Maximizing conjunctive use of surface and ground water under surface water quality constraints. *Adv. Water Resour.* **1995**, *18*, 67–75. [[CrossRef](#)]
8. Başağaoğlu, H.; Mariño, M.A. Joint management of surface and ground water supplies. *Ground Water* **1999**, *37*, 214–222. [[CrossRef](#)]
9. Azaiez, M.N. A model for conjunctive use of ground and surface water with opportunity costs. *Eur. J. Oper. Res.* **2002**, *143*, 611–624. [[CrossRef](#)]
10. Mohan, S.; Jothiprakash, V. Development of priority-based policies for conjunctive use of surface and groundwater. *Water Int.* **2003**, *28*, 254–267. [[CrossRef](#)]
11. Pulido-Velazquez, D.; Ahlfeld, D.; Andreu, J.; Sahuquillo, A. Reducing the computational cost of unconfined groundwater flow in conjunctive-use models at basin scale assuming linear behaviour: The case of Adra-Campo de Dalías. *J. Hydrol.* **2008**, *353*, 159–174. [[CrossRef](#)]
12. Matrosov, E.S.; Harou, J.J.; Loucks, D.P. A computationally efficient open-source water resource system simulator—Application to London and the Thames Basin. *Environ. Modell. Softw.* **2011**, *26*, 1599–1610. [[CrossRef](#)]
13. Shi, F.; Zhao, C.; Sun, D.; Peng, D.; Han, M. Conjunctive use of surface and groundwater in central Asia area: A case study of the Tailan River Basin. *Stoch. Environ. Res. Risk Assess.* **2012**, *26*, 961–970. [[CrossRef](#)]
14. Bejranonda, W.; Koch, M.; Koontanakulvong, S. Surface water and groundwater dynamic interaction models as guiding tools for optimal conjunctive water use policies in the central plain of Thailand. *Environ. Earth Sci.* **2013**, *70*, 2079–2086. [[CrossRef](#)]
15. Khan, M.; Voss, C.; Yu, W.; Michael, H. Water resources management in the Ganges Basin: A comparison of three strategies for conjunctive use of groundwater and surface water. *Water Resour. Manag.* **2014**, *28*, 1235–1250. [[CrossRef](#)]
16. The World Bank, Water for Food Team. *Conjunctive Use of Groundwater and Surface Water; Agricultural and Rural Development Notes, Issue 6*; The World Bank: Washington, DC, USA, 2006.
17. Safavi, H.R.; Rezaei, F. Conjunctive use of surface and ground water using fuzzy neural network and genetic algorithm. *Iran. J. Sci. Technol.-Trans. Civ. Eng.* **2015**, *39*, 365–377.
18. Zhang, L.; Zhang, J.; Wu, Z. Advance on conjunctive operation of surface water and groundwater. *Desalination Water Treat.* **2013**, *52*, 1956–1964. [[CrossRef](#)]
19. Zhou, Y.; Herath, H.M.P.S.D. Evaluation of alternative conceptual models for groundwater modelling. *Geosci. Front.* **2017**, *8*, 437–443. [[CrossRef](#)]
20. Anderson, M.P.; Woessner, W.W. *Applied Groundwater Modeling—Simulation of Flow and Advective Transport*; Academic Press Inc.: San Diego, CA, USA, 1992; 381p.
21. Izady, A.; Davary, K.; Alizadeh, A.; Ziaei, A.N.; Alipour, A.; Joodavi, A.; Brusseau, M.L. A framework toward developing a groundwater conceptual model. *Arab. J. Geosci.* **2014**, *7*, 3611–3631. [[CrossRef](#)]
22. Betancur, T.; Palacio, C.A.; Escobar, J.F. Conceptual Models in Hydrogeology. Methodology and Results. In *Hydrogeology—A Global Perspective*; Kazemi, G.A., Ed.; InTechOpen: London, UK, 2012; 232p, ISBN 978-953-51-0048-5.
23. Betancur, T. Una Aproximación al Conocimiento de un Sistema Acuífero Tropical. Caso de Estudio: Bajo Cauca Antioqueño. Ph.D. Thesis, Universidad de Antioquia, Medellín, Colombia, 2008; 221p.
24. Singhal, V.; Goyal, R. Development of conceptual groundwater flow model for Pali Area, India. *Afr. J. Environ. Sci. Technol.* **2011**, *5*, 1085–1092. [[CrossRef](#)]
25. Watkins, D.W.; McKinney, D.C.; Maidment, D.R. Use of geographic information systems in ground-water flow modeling. *J. Water Resour. Plann. Manag.* **1996**, *122*, 88–96. [[CrossRef](#)]
26. Gkiouggkis, I.; Pouliaris, C.; Pliakas, F.-K.; Diamantis, I.; Kallioras, A. Conceptual and Mathematical Modeling of a Coastal Aquifer in Eastern Delta of R. Nestos (N. Greece). *Hydrology* **2021**, *8*, 23. [[CrossRef](#)]
27. Bear, J.; Beljin, M.S.; Ross, R.R. *Fundamentals of Ground-Water Modeling*; Ground Water Issue; EPA/540/S-92/005; United States Environmental Protection Agency, Office of Solid Waste and Emergency, Response Office of Research and Development: Washington, DC, USA, 1992.
28. Zeng, X.; Wang, D.; Wu, J.; Chen, X. Reliability Analysis of the Groundwater Conceptual Model. *Hum. Ecol. Risk Assess. Int. J.* **2013**, *19*, 515–525. [[CrossRef](#)]
29. Poeter, E.; Anderson, D. Multimodel ranking and inference in ground water modeling. *Ground Water* **2005**, *43*, 597–605. [[CrossRef](#)] [[PubMed](#)]
30. Rojas, R.; Feyen, L.; Dassargues, A. Conceptual model uncertainty in groundwater modeling: Combining generalized likelihood uncertainty estimation and Bayesian model averaging. *Water Resour. Res.* **2008**, *44*, W12418. [[CrossRef](#)]
31. Delimani, P. Geological Changes of the Coastline in the Thrace Region and Impact on the Land Use of the Coastal Zone. Ph.D. Thesis, Department of Civil Engineering, Democritus University of Thrace, Xanthi, Greece, 2000. (In Greek)
32. Gkiouggkis, I. Investigation of Marine Intrusion in Coastal Aquifers in Deltaic Environment. The Case of Nestos River Delta. Ph.D. Thesis, Department of Civil Engineering, Democritus University of Thrace, Xanthi, Greece, 2018. (In Greek)
33. Institute of Geological and Mineral Exploration—IGME. *Geological Map of Greece, 1:50,000, Chrisoupolis Sheet*; IGME: Athens, Greece, 1982.
34. Diamantis, I.; Petalas, C.; Tzevelekis, T.; Pliakas, F. Investigation of water supply potential for coastal settlements in Thrace by coastal aquifers. In *Technical Report to the East Macedonia and Thrace Region*; Greece, 1994; Volume 4, 393p. (In Greek)

-
35. Piper, A.M. A graphic procedure in the geochemical interpretation of water-analyses. *Eos Trans. Am. Geophys. Union* **1944**, *25*, 914–928. [[CrossRef](#)]
 36. Kampas, G.; Diamantis, I.; Panagopoulos, A.; Pliakas, F.-K. Groundwater conceptual model development in the River Nestos Western Delta, NE Greece. In *Proceedings of the 12th International Hydrogeological Conference, Nicosia, Cyprus, 20–22 March 2022*; pp. 112–114.